Chapter 7
Viscoplastic Behaviour of the Heat-Affected Zone in TIG-Welded 6005 Aluminum

M. Sasso, M. Utzeri, G. Chiappini, M. Rossi, and A. Perticone

Abstract This work investigates the mechanical behavior of TIG-welded AA6005-T6 aluminum alloy by combining experimental testing and numerical modeling to achieve a deeper understanding of the welding-induced mechanical modifications. The study was carried out within the collaboration between Università Politecnica delle Marche and Hitachi Rail STS company. From an experimental point of view, tensile tests were performed both on standard specimens and on customized geometries to assess the local mechanical response across the different zones affected by the welding process. Full-field strain measurements were acquired by means of Digital Image Correlation (DIC), that allowed detailed monitoring of strain evolution during loading. The results revealed a significant loss of strength within the heat-affected zone (HAZ), confirming the tendency of deformation and fracture to localize in this region due to modification of microstructure induced by welding. In parallel, a finite element (FEM) model was developed using Abaqus to simulate the response of the welded joint. In the first stage, the model was defined with three discrete regions—base material, HAZ, and weld bead—each assigned specific mechanical properties. In a subsequent phase, a more realistic continuous property approach was implemented, introducing a gradual variation of material parameters along the welded area to represent the mechanical gradient generated by the thermal cycle. The FEM models were calibrated using the Voce hardening law to describe the plastic behavior of the material, showing improved agreement with the experimental data when adopting the continuous property formulation. Model validation demonstrated an overall good consistency between simulations and experiments, despite some discrepancies attributed to local variations in sheet thickness, uncertainties in the exact weld bead position, voids and welding defects.

Keyword Heat-affected Zone · viscoplasticity · welded aluminum

Introduction

Aluminum alloys are widely employed in aerospace, automotive, and transportation industries due to their high strength-to-weight ratio, corrosion resistance, and excellent formability [1]. Among them, the 6005T6 alloy is commonly used for structural components, particularly in applications where welding is required to assemble lightweight frameworks. While welding enables the creation of complex geometries and strong joints, it also introduces significant microstructural and mechanical heterogeneities [2]. The thermal cycles associated with welding produce localized changes in the material, most notably in the heat-affected zone (HAZ), where softening or reduced ductility can occur. These alterations can significantly affect the mechanical performance of welded structures, influencing load-bearing capacity, ductility, and failure modes under both quasi-static and high-strain-rate conditions [3]. Understanding the mechanical behavior of welded aluminum sheets

M. Sasso · M. Utzeri · M. Rossi
Marche Polytechnic University, DIISM, Ancona (IT)
e-mail: m.sasso@univpm.it; m.utzeri@univpm.it; m.rossi@univpm.it

G. Chiappini
eCampus University, Novedrate (IT)
e-mail: gianluca.chiappini@uniecampus.it

A. Perticone
Hitachi Rail STS Spa, Pistoia (IT)
e-mail: alberto.perticone.ayes@hitachirail.com

© The Author(s), under exclusive license to River Publishers 2026

Paul Allison et al. (eds.), *Dynamic Behavior of Materials, Volume 1, 2026*, Conference Proceedings of the Society for Experimental Mechanics Series, https://doi.org/10.13052/rp-9788743816249

requires detailed experimental characterization as well as robust numerical modeling. Traditional quasi-static tensile and bending tests provide fundamental insights into elastic-plastic response, ultimate strength, and strain localization. However, real-world structures often experience dynamic or impact loading, where strain-rate sensitivity and inertia effects play a critical role. In such cases, high-speed experimental techniques, including Split Hopkinson Pressure Bar (SHPB) testing, allow the measurement of material response at strain rates up to 10^3 s^{-1} [4]. Complementary digital image correlation (DIC) provides full-field strain measurements, enabling detailed evaluation of strain localization, especially in the HAZ and weld bead. Numerical modeling is essential for extrapolating experimental results and for predictive design purposes. Finite element simulations allow detailed investigation of local stress and strain distributions in welded joints, incorporating both base metal and welded regions. Accurate representation of the HAZ is particularly challenging due to its heterogeneous properties. Approaches based on equivalent material models, calibrated using experimental stress–strain curves, can effectively reproduce macroscopic response while maintaining computational efficiency. Moreover, constitutive models that account for strain-rate sensitivity, such as the Johnson–Cook law [5], are critical for dynamic simulations, while ductile fracture criteria, including the Bao–Wierzbicki approach, enable reliable estimation of strain to failure under varying stress states and strain rates [6]. In addition to standard unnotched specimens, the evaluation of notched and shear specimens provides insight into the effects of stress triaxiality and geometrical discontinuities on failure behavior. Notched samples highlight regions prone to strain localization, particularly in the HAZ, while shear tests assess joint performance under complex stress states. Combining experimental characterization of these different configurations with numerical modeling allows validation of material parameters and evaluation of predictive capabilities under both quasi-static and dynamic conditions. The present study focuses on TIG-welded 6005T6 aluminum sheets with a nominal thickness of 4 mm, systematically investigating their mechanical behavior under various loading conditions. By integrating experimental results from tensile, notched, and shear specimens with finite element simulations incorporating equivalent HAZ properties, Johnson–Cook strain-rate sensitivity, and Bao–Wierzbicki fracture criteria, this work aims to provide a comprehensive framework for predicting macroscopic performance. The findings offer insights into strain localization, strain-to-failure behavior, and the influence of stress triaxiality, supporting improved design, assessment, and optimization of welded aluminum structures.

Materials and Methods

The study focused on evaluating the mechanical behavior of welded aluminum sheets under both quasi-static and dynamic loading conditions. The base material consisted of commercially available aluminum alloy sheets 6005T6, with 4.0 mm nominal thickness, which were cut into rectangular coupons using a precision shearing machine to minimize edge deformation. Prior to welding, all sheets were degreased with acetone and cleaned with ethanol to remove surface contaminants and oxide layers. Sheets were then aligned in a butt-joint configuration with no overlap and clamped firmly to prevent misalignment or warping during welding. Welding was carried out using a Gas Tungsten Arc Welding (GTAW/TIG) process with a pulsed current to reduce heat input while ensuring complete joint fusion. Filler material matching the base alloy composition was employed for metallurgical consistency. After welding, specimens cooled naturally at room temperature to minimize residual stresses. Post-welding, the specimens were obtained by means of water-jetting process following geometries suitable for tensile tests: specimen for uniaxial stress state (P), notched specimens for triaxial stress state (N), and Driemeier sample for shear stress state (D). Figure 1 summarizes the chosen sample shapes. Waterjet ensured precise dimensions, reduced thermal effect on welded region (compared to laser cutting), and uniform cross-sectional areas. Specimens were oriented so that the weld seam was normal to the gauge length in tensile tests and parallel to the loading direction in shear test. Quasi-static tensile tests were conducted using a universal testing machine at strain rates ranging from 10^{-3} s^{-1} to 10^{-1} s^{-1}. Load and displacement were recorded continuously, and strain was measured using Digital Image Correlation technique (DIC) [7]. For dynamic testing, a Split Hopkinson Pressure Bar (SHPB) setup was employed, enabling the investigation of material response at high strain rates ($\approx 10^2$–10^3 s^{-1}), more details are provided in previous works [8]. Specimens were positioned between incident and transmitted steel bars and the experimental tests were recorded at 125000 Hz with a Photron Fastcam S4.

Numerical Modelling

A finite element model was developed to simulate the mechanical response of welded aluminum sheets under both quasi-static and dynamic loading conditions. The specimen geometry reproduced the experimental dimensions, including the welded lap joint, and the model distinguished two regions: the unwelded base metal, the welded zone which includes both

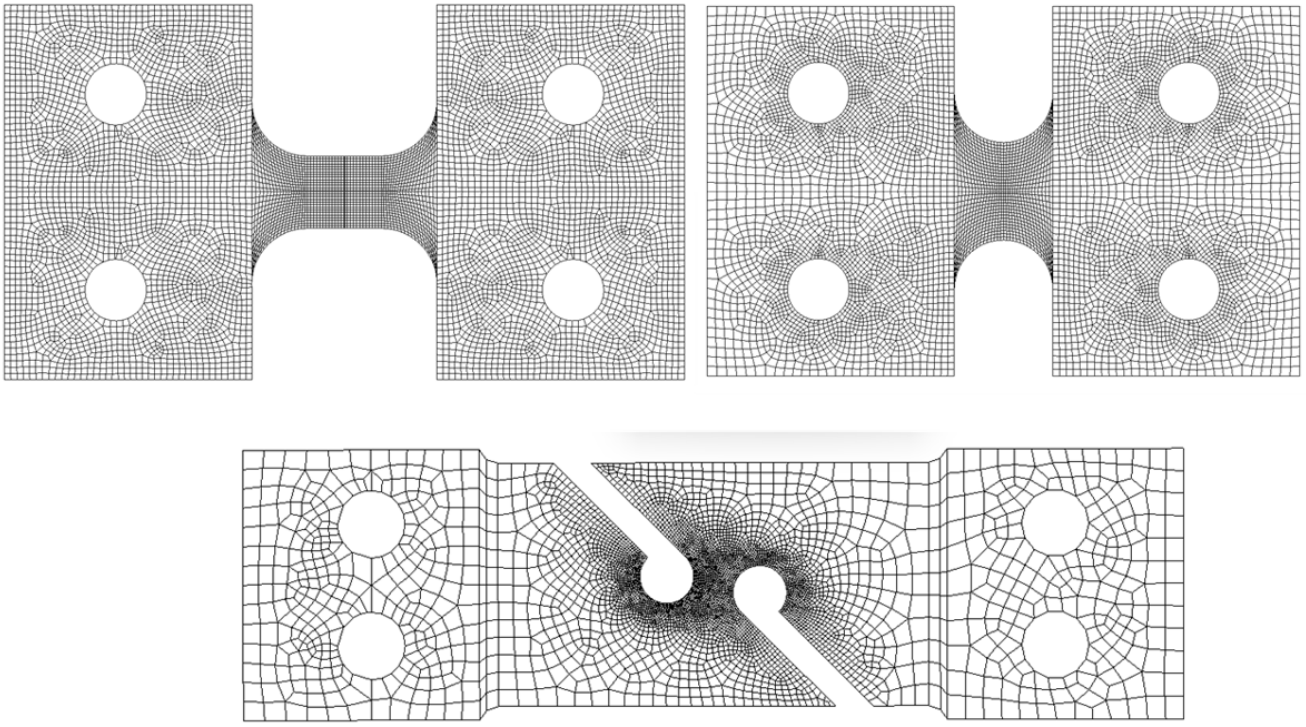

Fig. 1 Sample specimens for quasi-static and high strain rate test: smooth, notched and Driemeier shapes.

weld seam (fusion zone) and heat-affected zones (HAZ). This partitioning allowed the assignment of distinct material behaviors to capture local variations in strength, ductility, and strain-rate sensitivity induced by the welding process. For the base metal, the material was represented using a classical isotropic von Mises yield criterion, calibrated from tensile tests on unmodified aluminum 6005T6 sheets. Elastic properties were assigned according to standard alloy data, while plastic behavior was described using a Voce hardening law derived from experimental stress–strain responses. This approach ensured accurate reproduction of the elastic-plastic behavior in unwelded regions under low strain rates. For dynamic simulations, particularly those replicating Split Hopkinson Pressure Bar (SHPB) tests, the base metal was modeled using the Johnson–Cook multiplier to account for strain-rate sensitivity and thermal effects. The welded region, including the fusion zone and HAZ, was modeled as an equivalent homogenized material with a length of 50 mm. Material parameters for this zone were derived from calibration procedure to reproduce an equivalent stress–strain response observed in welded specimens. The model incorporated Voce hardening law with Johnson–Cook multiplier to account for strain-rate effects across the weld and HAZ. Boundary conditions in the numerical model mirrored the experimental setups: displacement-controlled loading for quasi-static tests and strain-rate-controlled inputs for SHPB simulations. The mesh was refined in the 50 mm welded (HAZ and weld seam) region to resolve stress and strain gradients, while coarser elements were used in the base metal to optimize computational cost. A comprehensive sketch of geometrical model over experimental samples was provided in Figure 2. Model outputs included engineering stress–strain fields, overall load-displacement curves, and the evolution of plastic deformation, enabling direct comparison with experimental results and validation of the equivalent material approach for welded regions under both low- and high-rate loading conditions. To accurately capture the onset of failure, the model incorporates a failure criterion based on the Bao–Wierzbicki approach. The critical equivalent plastic strain (ε_f) was determined by monitoring the numerical simulation until complete fracture of the specimen. The Bao–Wierzbicki model allows ε_f to depend on local stress triaxiality and strain rate, providing a more realistic representation of ductile fracture in the homogenized region. This approach ensures that the numerical predictions only reproduce the load–displacement response; the mode of crack initiation and propagation were not predictable because the local change in mechanical properties in real experiments. ε_f values were calibrated by iteratively adjusting model parameters to match the experimentally observed failure points in both quasi-static and dynamic tests.

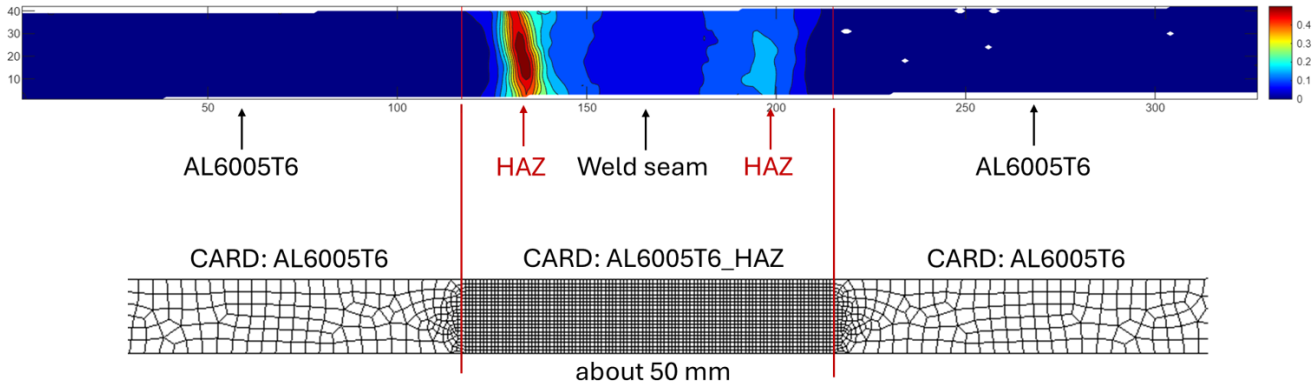

Fig. 2 Sketch of welded region and numerical model implemented.

Results and Discussion

A primary objective of the numerical modeling was to accurately represent the mechanical response of HAZ region with a single material model, which is known to exhibit altered mechanical properties due to thermal cycles during welding. The experimental stress–strain curves obtained from tensile tests on welded specimens showed a characteristic reduction in ductility and, in some cases, a slight decrease in yield strength within the HAZ compared to the base metal. This behavior was successfully captured by the equivalent material approach implemented in the finite element model, in which homogeneous properties were assigned to the welded zone. As shown in Figure 3, the simulated stress–strain response of the HAZ closely follows the experimental curve in both the elastic and early plastic regions, indicating that the calibrated yield stress and hardening parameters adequately represent the local mechanical behavior.

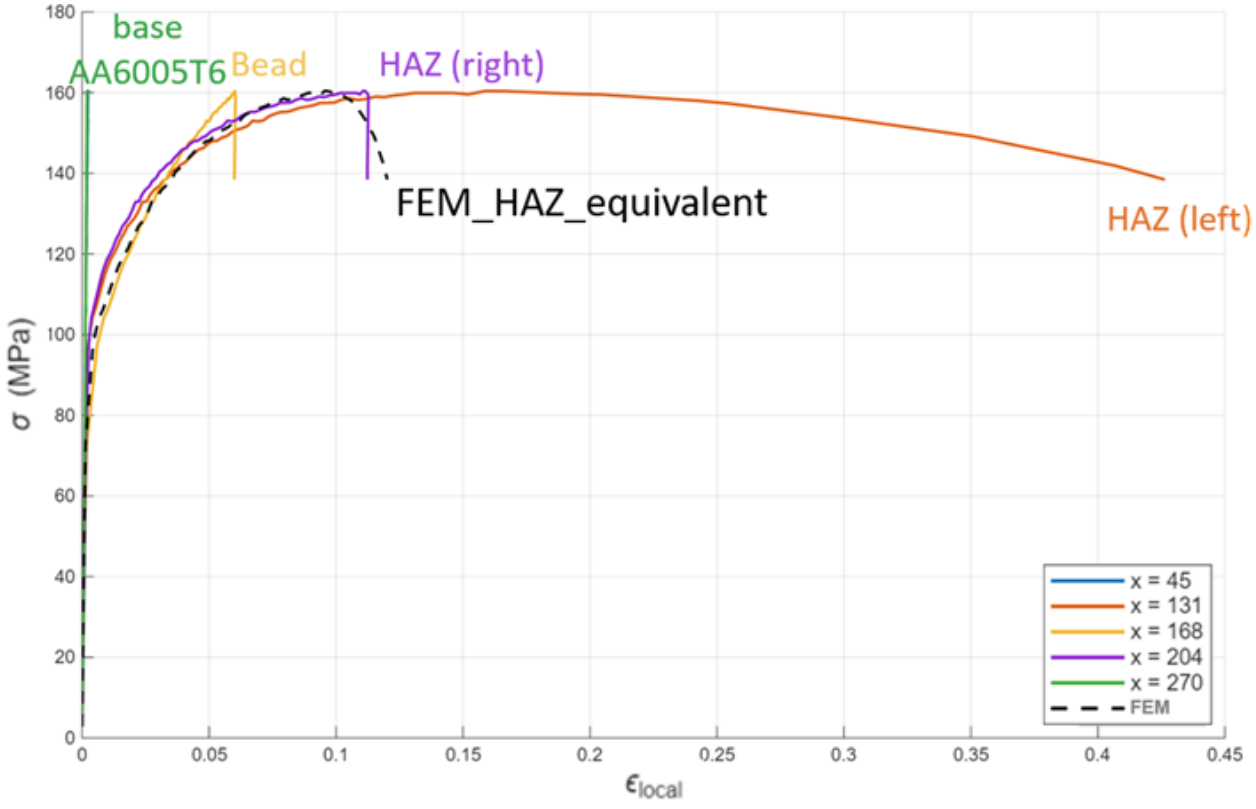

Fig. 3 Stress-strain response of homogeneous material model versus local stress-strain curves.

Table 1 Voce and Johnson Cook material model of welded region

σ_0 [MPa]	R_0 [MPa]	b [-]	$\dot{\varepsilon}_0$ [1/s]	C [-]	E [MPa]	ν [-]
96	92	22	0.1	0.021	69000	0.3

The comparison demonstrates that the homogenized HAZ approach can effectively capture the overall mechanical response up to moderate strain. At large strain the stress-strain curve locally increases because of the extended ductility of the local HAZ region. That specific localization could not be appreciated by the homogeneous material model due to the constant mechanical properties across the weld region. Despite differences at large strain, the predicted ultimate load and corresponding displacement are consistent with the experimental values, demonstrating the model's reliability for quasi-static design purposes. Under dynamic loading, the experimental results indicate a clear strain-rate sensitivity of the welded aluminum sheets, with both the yield stress and ultimate tensile strength increasing with higher loading rates, while the total elongation seems not to be influenced as shown in Figure 4.

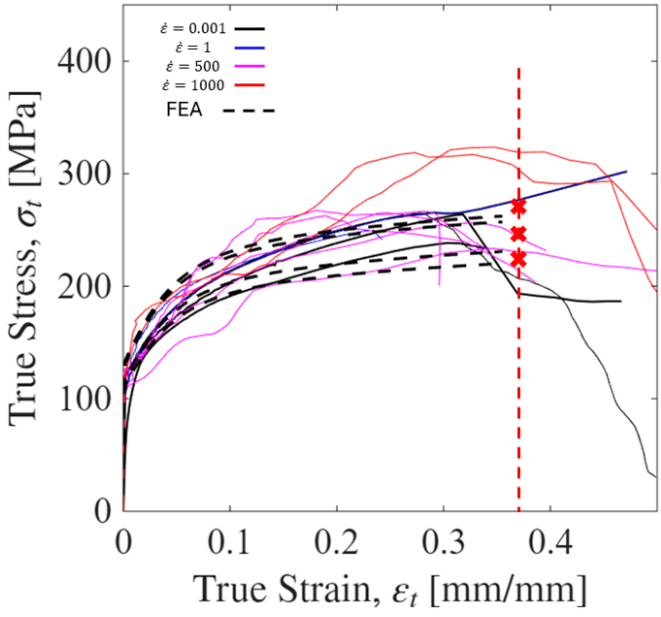

Fig. 4 Numerical vs experimental stress-strain response of smooth samples under quasi-static and dynamic loading conditions.

The finite element model incorporating the Johnson–Cook constitutive law successfully reproduced these trends. Figure 4 illustrates the stress–strain curves obtained at different strain rates, showing that the model captures the increasing strength and rate-dependent hardening observed in the experiments. The final material parameters are summarized in Table 1.

To evaluate the effect of stress concentrations on welded aluminum sheets, tensile tests were conducted on notched specimens. Both quasi-static and dynamic tests were performed to investigate how the heat-affected zone (HAZ) and weld bead respond under localized high stresses. Experimental results showed that cracks consistently initiated at the notch root, with higher strains of local failure than smooth specimens (P). In dynamic tests, the notched specimens exhibit a strain-rate sensitivity according to the uniaxial stress state without a clear effect on strain to failure, reflecting the combined influence of strain-rate sensitivity and stress concentration. The HAZ adjacent to the weld was the critical region for crack initiation, consistent with observations from unnotched specimens. Using the Johnson–Cook law for dynamic loading and calibrated HAZ properties for quasi-static tests, simulations predicted peak stresses and strain localization patterns in good agreement with experiments. The notch root was correctly identified as the primary failure site. The comparison between the numerical and experimental load-displacement curves is shown in Figure 5.

Strain to failure is a critical parameter for evaluating the ductility and failure modes of welded aluminum sheets. In the experiments, failure in the quasi-static tensile tests typically initiated in the HAZ, where the combination of lower ductility and stress concentration near the fusion line promotes localized necking and crack formation. The ε_f values computed with the Bao–Wierzbicki criterion showed good agreement with the experimental fracture strains. Figure 6 presents the

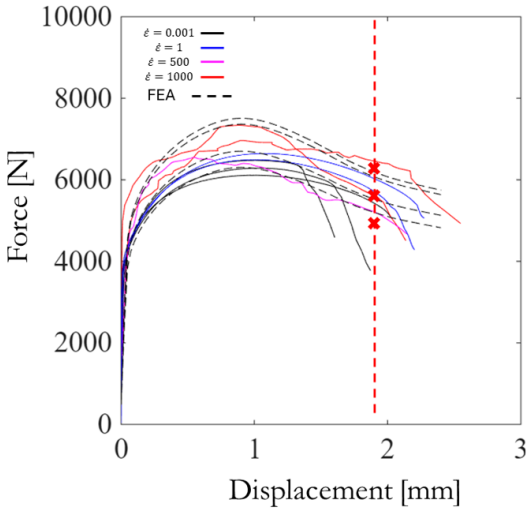

Fig. 5 Numerical vs experimental load-displacement response of nothced samples under quasi-static and dynamic loading conditions.

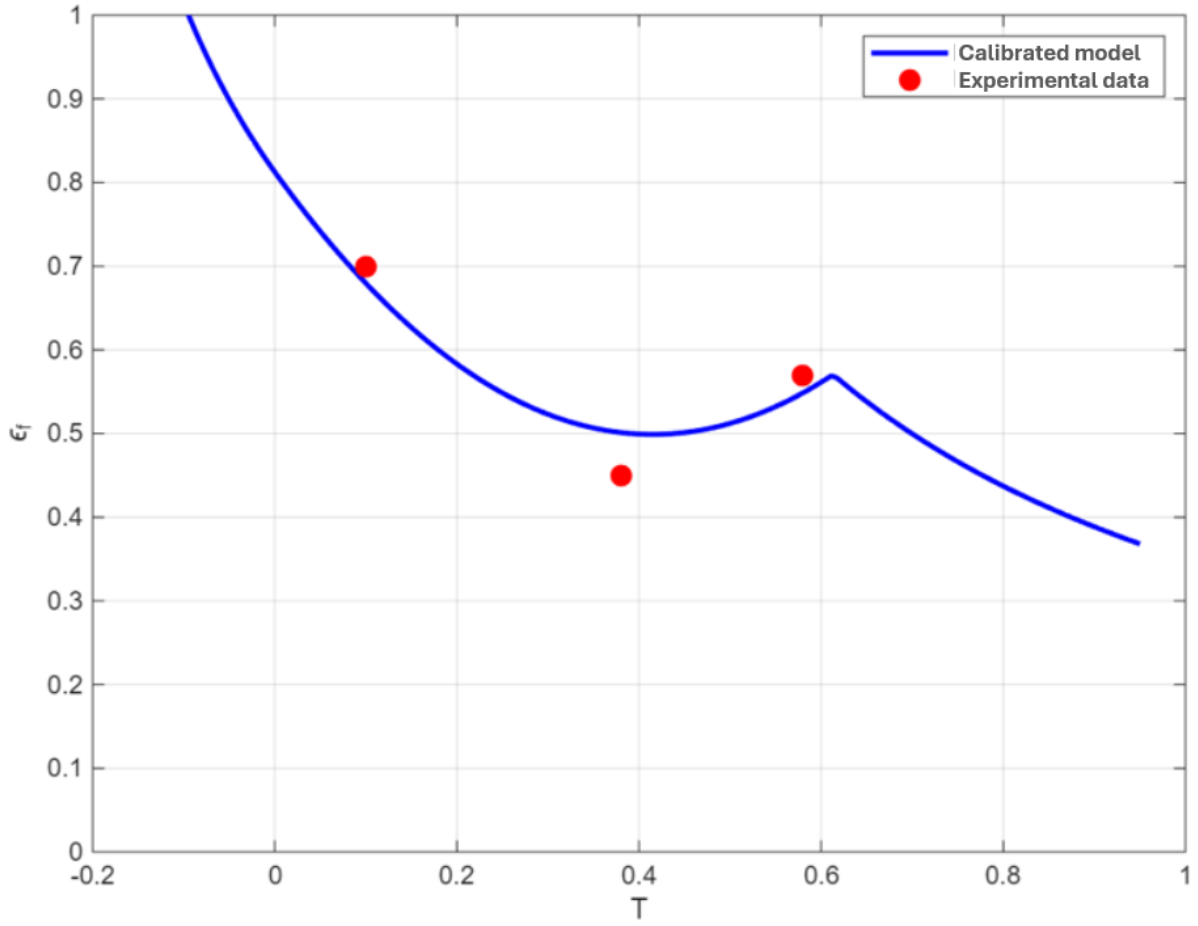

Fig. 6 Fracture locus of homogeneus material model representing the welded region.

comparison between the numerically predicted strain at failure and the measured deformation in the welded specimens. The model does not identify the correct site of crack initiation but reproduces the reduced ductility observed experimentally with consistent load-displacement curve in tensile, notched and Driemeier samples. In dynamic tests, the strain to failure

is not affected by the high strain rates so only the effect of stress triaxiality was considered, and the numerical predictions closely follow this trend. This confirms that the Bao–Wierzbicki approach provides a reliable framework for predicting the macroscopic failure of welded aluminum sheets under both low- and high-rate loading conditions.

Conclusion and Future Work

The combined experimental and numerical investigation demonstrates that a homogenized HAZ model can effectively reproduce the macroscopic mechanical response of welded 6005T6 aluminum sheets under quasi-static and dynamic loading. The finite element model, calibrated using the Bao–Wierzbicki fracture criterion and Johnson–Cook constitutive law, accurately predicts strain to failure and load–displacement behavior for smooth, notched, and shear specimens. Strain-rate sensitivity is captured in dynamic tests, while stress triaxiality dominates failure in notched samples. Overall, the approach provides a robust framework for predicting macroscopic behavior and assessing welded aluminum structures, offering valuable guidance for design, safety evaluation, and optimization of welded components.

References

1. Ding H, Zhu T, Zhang J, et al (2026) Constitutive and fracture models for metallic materials with applications to rail vehicle collisions: An overview. Thin-Walled Structures 219:114280. https://doi.org/10.1016/j.tws.2025.114280
2. Costas M, Morin D, Hopperstad OS, et al (2019) A through-thickness damage regularisation scheme for shell elements subjected to severe bending and membrane deformations. Journal of the Mechanics and Physics of Solids 123:190–206. https://doi.org/10.1016/j.jmps.2018.08.002
3. Woelke PB, Hiriyur BK, Nahshon K, Hutchinson JW (2017) A practical approach to modeling aluminum weld fracture for structural applications. Engineering Fracture Mechanics 175:72–85. https://doi.org/10.1016/j.engfracmech.2017.02.010
4. Utzeri M, Farotti E, Coccia M, et al (2021) High strain rate compression behaviour of 3D printed Carbon-PA. Journal of Materials Research 36:2083–2093. https://doi.org/10.1557/s43578-021-00248-9
5. Utzeri M, Bhagavatam A, Mancini E, et al (2021) Quasi-Static and Dynamic Behavior of Inconel 625 Obtained by Laser Metal Deposition: Experimental Characterization and Constitutive Modeling. Journal of Engineering Materials and Technology 143:041007. https://doi.org/10.1115/1.4051087
6. Bao G, Wierzbicki T (2004) On fracture locus in the equivalent strain and stress triaxiality space. Int J Mech Sci 36:81–98. https://doi.org/:10.1016/j.ijmecsci.2004.02.006
7. Sasso M, Mancini E, Chiappini G, et al (2018) Application of DIC to Static and Dynamic Testing of Agglomerated Cork Material. Exp Mech 58:1017–1033. https://doi.org/10.1007/s11340-017-0369-9
8. Sasso M, Mancini E, Chiappini G, et al (2024) A 90-meter Split Hopkinson Tension–Torsion Bar: Design, Construction and First Tests. J dynamic behavior mater. https://doi.org/10.1007/s40870-024-00432-y